

# Triniobium Polytungstophosphates. Syntheses, Structures, Clarification of Isomerism and Reactivity in the Presence of H<sub>2</sub>O<sub>2</sub>

Mason K. Harrup, Gyu-Shik Kim,<sup>†</sup> Huadong Zeng, Rhoma P. Johnson, Don VanDerveer,<sup>‡</sup> and Craig L. Hill\*

Department of Chemistry, Emory University, Atlanta, Georgia 30322

Received April 24, 1998

The reaction of K<sub>7</sub>[HNb<sub>6</sub>O<sub>19</sub>], H<sub>2</sub>O<sub>2</sub> and A-Na<sub>9</sub>[PW<sub>9</sub>O<sub>34</sub>] in water followed by treatment with Cs<sup>+</sup> or (*n*-Bu<sub>4</sub>N)<sup>+</sup> (TBA) affords the corresponding salts of the tris(peroxoniobium) heteropolyanion A,β-[(NbO<sub>2</sub>)<sub>3</sub>PW<sub>9</sub>O<sub>37</sub>]<sup>6-</sup> (**1**) in ~60% isolated yields. An X-ray structure of the Cs salt, Cs**1** (monoclinic *P2/c*; *a* = 16.92360(10) Å, *b* = 13.5721(2) Å, *c* = 22.31890(10) Å, β = 92.0460(10)°, and *Z* = 4) confirms the A-type substitution pattern of the three Nb atoms and clarifies the M<sub>3</sub> rotational (Baker–Figgis) isomerism in the Keggin unit as β. The three terminal η<sup>2</sup>-O<sub>2</sub><sup>2-</sup> groups on the Nb atoms give **1** an overall symmetry approximating the chiral C<sub>3</sub>. These terminal peroxo ligands, and these groups only, thermally decompose when either Cs**1** or TBA**1** is in solution unless additional H<sub>2</sub>O<sub>2</sub> is present. The peroxo groups can be titrated with triphenylphosphine (2.8 ± 0.3 peroxide groups found per molecule). Refluxing TBA**1** in acetonitrile for 24 h in the presence of base generates the parent heteropolyanion, [Nb<sub>3</sub>PW<sub>9</sub>O<sub>40</sub>]<sup>6-</sup> (**2**) in 80% yield after isolation. Treatment of **2** with glacial acetic acid in acetonitrile converts it to [Nb<sub>6</sub>P<sub>2</sub>W<sub>18</sub>O<sub>77</sub>]<sup>6-</sup> (**3**) in ~100% yield, while treatment of TBA**3** with hydroxide converts it back to **2** in high yield. Spectroscopic (FTIR, Raman, <sup>183</sup>W NMR, and <sup>31</sup>P NMR), titrimetric, mass spectrometric (FABMS), and elemental analysis data are all consistent with these formulas. The addition of TBA**1** to solutions of alkenes and 33% aqueous peroxide in acetonitrile at reflux results in the generation of the corresponding vicinal diols in high selectivity and yield at high conversion of substrate. Several spectroscopic and kinetics experiments, including a novel one correlating the incubation time of TBA**1** under the reaction conditions with the rates of alkene oxidation, establish that TBA**1** functions primarily as a catalyst precursor and that much of the catalytic activity is derived from generation of tungstate under the reaction conditions.

## Introduction

The substitution of Nb<sup>V</sup> for W<sup>VI</sup> or Mo<sup>VI</sup> in polyoxometalates (POMs) increases the negative charge on the complexes, rendering them more basic and reactive (nucleophilic) toward many organometallic or organic groups and more stable in neutral and basic media.<sup>1,2</sup> Key efforts include the preparation, physical characterization, and chemistry of the Nb-substituted heteropolyanions [Nb<sub>3</sub>SiW<sub>9</sub>O<sub>40</sub>]<sup>7-</sup>, its dimeric form [Nb<sub>6</sub>Si<sub>2</sub>W<sub>18</sub>O<sub>77</sub>]<sup>8-,3-6</sup> and [Nb<sub>3</sub>P<sub>2</sub>W<sub>15</sub>O<sub>62</sub>]<sup>9-7-10</sup> by the Finke group and similar extensive efforts with the Nb-substituted

isopolyanion C<sub>2v</sub>-[Nb<sub>2</sub>W<sub>4</sub>O<sub>19</sub>]<sup>4-</sup> by the Klemperer and Day groups.<sup>11–14</sup> A major thrust of both groups was the use of these high charge density polyanions as limited-domain close-packed polyoxide supports for organometallic units.

Research in two areas involving the attractive features conferred by the substitution of Nb in POMs has provided the impetus for the present study. First, recent research from our group<sup>15–18</sup> and others<sup>19</sup> has established that Nb derivatives of POMs are more active as antiviral agents and less toxic both in vitro and in vivo than the parent Nb-free POMs.<sup>20</sup> Second (the

\* To whom correspondence should be addressed. Fax: (404) 727-6076. E-mail: chill@emory.edu.

<sup>†</sup> Permanent address: Department of Science Education, Kangwon National University, Chunchon 200-701, Korea.

<sup>‡</sup> School of Chemistry and Biochemistry, Georgia Institute of Technology, Atlanta, GA 30332.

- (1) Recent reviews on polyoxometalates: (a) Pope, M. T.; Müller, A. *Angew. Chem., Int. Ed. Engl.* **1991**, *30*, 34–48. (b) *Chem. Rev.* **1998**, *98*, 1–390 (Special Issue on Polyoxometalates; Hill, C. L., Ed.).
- (2) Review of organometallic and organic derivatives of POMs: Gouzerh, P.; Proust, A. *Chem. Rev.* **1998**, *98*, 77–111.
- (3) Finke, R. G.; Droge, M. W. *J. Am. Chem. Soc.* **1984**, *106*, 7274–7277.
- (4) Edlund, D. J.; Saxton, R. J.; Lyon, D. K.; Finke, R. G. *Organometallics* **1988**, *7*, 1692–1704.
- (5) Droge, M. W.; Finke, R. G. *J. Mol. Catal.* **1991**, *69*, 323–338.
- (6) Lin, Y.; Nomiya, K.; Finke, R. G. *Inorg. Chem.* **1993**, *32*, 6040–6045.
- (7) Lin, Y.; Finke, R. G. *Inorg. Chem.* **1994**, *33*, 4891–4910.
- (8) Lin, Y.; Finke, R. G. *J. Am. Chem. Soc.* **1994**, *116*, 8335–8353.
- (9) Pohl, M.; Lyon, D. K.; Mizuno, N.; Nomiya, K.; Finke, R. G. *Inorg. Chem.* **1995**, *34*, 1413–1429.
- (10) Finke, R. G.; Lyon, D. K.; Nomiya, K.; Weakley, T. J. R. *Acta Crystallogr.* **1990**, *C46*, 1592–1596 and references cited in each.

- (11) Besecker, C. J.; Klemperer, W. G.; Day, V. W. *J. Am. Chem. Soc.* **1982**, *104*, 6158–6159.
- (12) Besecker, C. J.; Day, V. W.; Klemperer, W. G.; Thompson, M. R. *J. Am. Chem. Soc.* **1984**, *106*, 4125–4136.
- (13) Besecker, C. J.; Day, V. W.; Klemperer, W. G.; Thompson, M. R. *Inorg. Chem.* **1985**, *24*, 44–50.
- (14) Day, V. W.; Klemperer, W. G.; Schwartz, C. *J. Am. Chem. Soc.* **1987**, *109*, 6030–6044.
- (15) Hill, C. L.; Judd, D.; Schinazi, R. F. Paper presented at the VIth International Antiviral Symposium, Nice, France, June 7–10, 1994.
- (16) Ni, L.; Boudinot, F. D.; Boudinot, S. G.; Henson, G. W.; Bossard, G. E.; Martelucci, S. A.; Ash, P. W.; Fricker, S. P.; Darkes, M. C.; Theobald, B. R. C.; Hill, C. L.; Schinazi, R. F. *Antimicrob. Agents Chemother.* **1994**, *38*, 504–510.
- (17) Kim, G.-S.; Judd, D. A.; Hill, C. L.; Schinazi, R. F. *J. Med. Chem.* **1994**, *37*, 816–20.
- (18) Hill, C. L.; Judd, D. A.; Tang, J.; Nettles, J.; Schinazi, R. F. *Antiviral Res.* **1997**, *34*, A43.
- (19) Yamamoto, N.; Schols, D.; De Clercq, E.; Debyser, Z.; Pauwels, R.; Balzarini, J.; Nakashima, H.; Baba, M.; Hosoya, M.; Snoeck, R.; Neyts, J.; Andrei, G.; Murrer, B. A.; Theobald, B.; Bossard, G.; Henson, G.; Abrams, M.; Picker, D. *Mol. Pharmacol.* **1992**, *42*, 1109–1117.
- (20) Rhule, J. T.; Hill, C. L.; Judd, D. A.; Schinazi, R. F. *Chem. Rev.* **1998**, *98*, 327–357.

main focus of this paper), it is clear that catalysis, and in particular the catalysis of selective oxidation processes by POMs or other species, in neutral or basic media is of considerable and growing interest.<sup>21–25</sup> Nearly all current POM-based catalytic oxidations including those of commercial and heterogeneous systems are slightly or strongly acidic in part as the dominant POM families sufficiently developed for such applications are only stable in acidic media.<sup>21,26</sup> The thermally unstable complex  $[(\text{NbO}_2)_6\text{P}_2\text{W}_{12}\text{O}_{56}]^{12-}$ , of interest in context with both antiviral and catalytic oxidation investigations, was characterized crystallographically, spectroscopically, and chemically.<sup>27</sup>

The current literature distinctly defines two dominant molecular roles for POMs in organic substrate oxidations based on the economically and environmentally attractive oxidant,  $\text{H}_2\text{O}_2$ : as precursors for polyperoxo catalysts, with the octa-peroxotetrametalates being the best characterized to date (chemistry primarily exhibited by  $\text{d}^0$  POMs),<sup>28–36</sup> and as intact catalysts for oxygenation (chemistry exhibited primarily by  $\text{d}$ -electron-ion-substituted POMs).<sup>37–40</sup> An example of the first category is the compound  $[(\text{NbO}_2)_3\text{SiW}_9\text{O}_{37}]^{7-}$ , whose synthesis, physical characterization, and  $\text{H}_2\text{O}_2$ -based oxidation chemistry were reported by Droegge and Finke.<sup>5</sup> These authors reported the product distributions from oxidation of several alkenes and preliminary rate law studies. From their rate law derived using initial rate kinetics,  $(-d[\text{allyl alcohol}]/dt)_0 = k[\text{allyl alcohol}][\text{H}_2\text{O}_2]^{1.4}[(\text{NbO}_2)_3\text{SiW}_9\text{O}_{37}]^{0.4}$ , they concluded, defensibly, that  $[(\text{NbO}_2)_3\text{SiW}_9\text{O}_{37}]^{7-}$  was not the active catalyst but that a fragment or fragments, and most probably  $\text{WO}_4^{2-}$ , were.

In this paper we report the synthesis and characterization of three phosphorus-centered triniobium Keggin analogues, the tris(peroxoniobium) monomer  $[(\text{NbO}_2)_3\text{PW}_9\text{O}_{37}]^{6-}$  (**1**), the corresponding tris(oxoniobium) monomer  $[\text{Nb}_3\text{PW}_9\text{O}_{40}]^{6-}$  (**2**), and the dimer  $[\text{Nb}_6\text{P}_2\text{W}_{18}\text{O}_{77}]^{6-}$  (**3**), and the X-ray structure of **Cs1**, which further clarifies the isomerism in **1** and related compounds prepared from  $\text{A}[\text{PW}_9\text{O}_{34}]^{9-}$ . In addition, product distribution and kinetics studies of alkene oxidations by  $\text{H}_2\text{O}_2$  in the presence of **1** are reported. We provide definitive evidence from a novel kinetic resolution catalyst decomposition study and conventional

experiments that **1** is not a significant catalyst but, as in the case of  $[(\text{NbO}_2)_3\text{SiW}_9\text{O}_{37}]^{7-}$ , fragments derived from **1** are.

## Experimental Section

**General Methods and Materials.** All chemicals used, including tetra-*n*-butylammonium (TBA) bromide, were commercially available reagent grade. Deionized water from a Barnstead single-stage deionizer (mixed-bed type) was used in all syntheses. All organic solvents used in the syntheses were ACS reagent grade, and the solvents used in catalytic reactions were B&J distilled-in-glass grade. The alkene substrates were ordered from Aldrich and used as received. The precursor polyoxometalates,  $\text{K}_7[\text{HNb}_6\text{O}_{19}]^{41}$  and  $\text{A-Na}_9[\text{PW}_9\text{O}_{34}]^{42}$  were synthesized and purified by literature procedures unless specified otherwise.<sup>43</sup> The tungstate used in the control experiments,  $(\text{TBA})_2\text{-WO}_4$ , was also synthesized by literature procedures.<sup>44</sup> Infrared spectra were obtained as KBr pellets (2–5 wt % of the sample) on a Nicolet 510M FTIR spectrophotometer. Raman spectra were obtained as solid samples on a Nicolet Raman 950 spectrophotometer equipped with a germanium detector. Fast atom bombardment mass spectra (FAB-MS) were obtained using a JEOL JMS-SX102/SX102A/E, five-sector, tandem mass spectrometer. The  $^{31}\text{P}$  NMR spectrum of the tris(peroxoniobium) complex, **1**, was recorded on an IBM WP-200SY FT spectrometer at 81.015 MHz. The  $^{183}\text{W}$  NMR spectrum of **TBA1** and the  $^{31}\text{P}$  NMR spectrum of **Cs1** [solubilized by lithiation ( $+\text{LiClO}_4$ ,  $-\text{CsClO}_4$ ) prior to data acquisition] were recorded on a Varian Unity 400 Plus spectrometer operating at 16.654 and 161.904 MHz, respectively. These  $^{31}\text{P}$  and  $^{183}\text{W}$  NMR spectra were run with 3 equiv of  $\text{H}_2\text{O}_2$  added to  $\text{CD}_3\text{CN}$  and  $\text{D}_2\text{O}$ , respectively, to stabilize **1**. While the presence of excess  $\text{H}_2\text{O}_2$  stabilizes the peroxo groups on **1**, it also leads to a slow degradation of the polytungstate unit, both processes that have been well documented in previous work (vide infra). The  $^{31}\text{P}$  NMR chemical shifts were referenced to 85%  $\text{H}_3\text{PO}_4$ , and the  $^{183}\text{W}$  NMR chemical shifts were referenced to 2.0 M  $\text{Na}_2\text{WO}_4$  in  $\text{D}_2\text{O}$ . Elemental analyses were conducted by E+R Microanalytical Laboratories.

All catalytic oxygenation reactions were analyzed by GC using an HP model 5890, fitted with a 25-m, 5% phenyl methyl silicone capillary column and a flame ionization detector, and by  $^1\text{H}$  NMR using a Nicolet NT-360 spectrometer at 361.037 MHz.

The concentration of unreacted  $\text{H}_2\text{O}_2$  in representative reactions was evaluated by iodometric titration.<sup>45</sup> A reasonably quantitative knowledge of the acidity was important in assessing epoxide ring opening during catalysis and other experiments. Unfortunately, however, pH is neither well defined nor readily evaluated by glass electrodes in nonaqueous media such as acetonitrile, the principal solvent in these studies. In response to this reality, two measurements were conducted to assess acidity. First, the acetonitrile solutions were dropped onto water-dampened pH paper, and second, both neutral  $\text{CH}_2\text{Cl}_2$  and a small portion of water were added to induce phase separation of the homogeneous acetonitrile solutions of polyoxometalate and the pH of the water layer was determined using a calibrated glass pH electrode. The measurements were in reasonable agreement, and as expected, the solutions were reasonably acidic (pH  $\sim$  2).

**Synthesis of  $(\text{TBA})_4\text{H}_2[(\text{NbO}_2)_3\text{PW}_9\text{O}_{37}]$  (**TBA1**).**  $\text{K}_7[\text{HNb}_6\text{O}_{19}] \cdot 13\text{H}_2\text{O}$  (1.5 g) was dissolved in a solution consisting of 10.0 mL of ca. 33% aqueous  $\text{H}_2\text{O}_2$  and 90.0 mL of water with moderate stirring.  $\text{HCl}$  (20 mL of 1.0 M solution) was added dropwise to give a yellow, effervescent solution. If the reaction solution became cloudy due to a suspension of  $\text{Nb}_2\text{O}_5$  prior to the addition of the lacunary polytungstophosphate, the solution was discarded.  $\text{A-Na}_9[\text{PW}_9\text{O}_{34}]$  (5.2 g) was immediately added, and stirring was continued for 15 min. At this

- (21) Hill, C. L.; Prosser-McCartha, C. M. *Coord. Chem. Rev.* **1995**, *143*, 407–455.
- (22) Parshall, G. W.; Ittel, S. D. *Homogeneous Catalysis. The Applications and Chemistry of Catalysis by Soluble Transition Metal Complexes*; 2nd ed.; Wiley-Interscience: New York, 1992.
- (23) Kozhevnikov, I. *Chem. Rev.* **1998**, *98*, 171–197.
- (24) Mizuno, N.; Misono, M. *Chem. Rev.* **1998**, *98*, 199–217.
- (25) Neumann, R. *Prog. Inorg. Chem.* **1998**, *47*, 317–370.
- (26) Okuhara, T.; Mizuno, N.; Misono, M. *Adv. Catal.* **1996**, *41*, 113–252.
- (27) Judd, D. A.; Chen, Q.; Campana, C. F.; Hill, C. L. *J. Am. Chem. Soc.* **1997**, *119*, 5461–5462.
- (28) Aubry, C.; Chottard, G.; Platzter, N.; Brégeault, J.-M.; Thouvenot, R.; Chauveau, F.; Huet, C.; Ledon, H. *Inorg. Chem.* **1991**, *30*, 4409–4415.
- (29) Salles, L.; Aubry, C.; Robert, F.; Chottard, G.; Thouvenot, R.; Ledon, H.; Brégeault, J.-M. *New J. Chem.* **1993**, *17*, 367–375.
- (30) Dengel, A. C.; Griffith, W. P.; Parkin, B. C. *J. Chem. Soc., Dalton Trans.* **1993**, 2683–2688.
- (31) Duncan, D. C.; Chambers, R. C.; Hecht, E.; Hill, C. L. *J. Am. Chem. Soc.* **1995**, *117*, 681–691.
- (32) Ishii, Y.; Yamawaki, K.; Yoshida, T.; Ura, T.; Ogawa, M. *J. Org. Chem.* **1987**, *52*, 1868–1870.
- (33) Ishii, Y.; Tanaka, H.; Nishiyama, Y. *Chem. Lett.* **1994**, 1–4.
- (34) Venturello, C.; D'Aloiso, R.; Bart, J. C.; Ricci, M. *J. Mol. Catal.* **1985**, *32*, 107–110.
- (35) Venturello, C.; D'Aloiso, R. *J. Org. Chem.* **1988**, *53*, 1553–1557.
- (36) Venturello, C.; Gambaro, M. *Synthesis* **1989**, *4*, 295–297.
- (37) Khenkin, A. M.; Hill, C. L. *Mendeleev Commun.* **1993**, 140–141.
- (38) Neumann, R.; Gara, M. *J. Am. Chem. Soc.* **1994**, *116*, 5509–5510.
- (39) Neumann, R.; Gara, M. *J. Am. Chem. Soc.* **1995**, *117*, 5066–5074.
- (40) Neumann, R.; Khenkin, A. M. *J. Mol. Catal. A: Chem.* **1996**, *114*, 169–180.

- (41) Dabbabi, M.; Boyer, M. *J. Inorg. Nucl. Chem.* **1976**, *38*, 1011–1014.
- (42) Massart, R.; Contant, R.; Fruchart, J.-M.; Ciabrini, J.-P.; Fournier, M. *Inorg. Chem.* **1977**, *16*, 2916–2921.
- (43) The initial precipitate of  $\text{A-Na}_9[\text{PW}_9\text{O}_{34}]$  was used without further purification.
- (44) Che, T. M.; Day, V. W.; Francesconi, L. C.; Fredrich, M. F.; Klemperer, W. G.; Shum, W. *Inorg. Chem.* **1985**, *24*, 4055–4062.
- (45) Day, R. A., Jr.; Underwood, A. L. *Quantitative Analysis*, 5th ed.; Prentice Hall: Englewood Cliffs, NJ, 1986; pp 1–774.

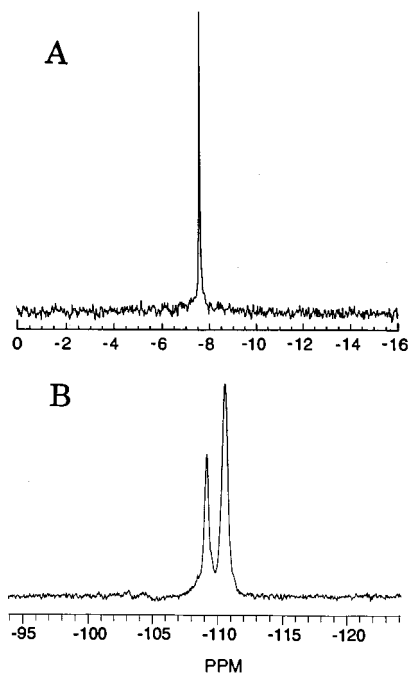


**Figure 1.** (A)  $^{31}\text{P}$  NMR (25 mM) and (B)  $^{183}\text{W}$  NMR (200 mM) spectra of TBA1. The  $^{31}\text{P}$  NMR spectrum was recorded in  $\text{CD}_3\text{CN}$  in the presence of aqueous  $\text{H}_2\text{O}_2$  (10% v/v ca. 33% aqueous  $\text{H}_2\text{O}_2$ ), and the  $^{183}\text{W}$  NMR spectrum was recorded in the presence of 3 equiv of  $\text{H}_2\text{O}_2$  in  $\text{CD}_3\text{CN}$ .

time, any insoluble material that remained was removed by filtration. To the filtrate was added 5.5 g of (TBA)Br, and the resulting yellow-orange precipitate was collected on a medium-porosity fritted Büchner funnel. The solid was then washed with three portions of water (10 mL) and allowed to air-dry for several hours. The dry solid was dissolved in 20 mL of acetonitrile, and any white insoluble solids were removed by filtration. The solvent was removed using a rotary evaporator. The resultant slightly tacky solid was then dissolved in 50 mL of methanol, and a yellow-white gel was removed by filtration. The volume of the filtrate was reduced by 20%, and the solution was stored at 0 °C for several hours. The product appeared as a bright yellow amorphous powder. The yield was approximately 5.0 g of product (59%).  $^{31}\text{P}$  NMR:  $\delta$  -7.86.  $^{183}\text{W}$  NMR:  $\delta$  -110.6 (6W), -109.2 (3W). The  $^{183}\text{W}$  NMR spectrum (see Figure 1) was obtained after only 7930 transients (<12 h). FTIR (1200–400  $\text{cm}^{-1}$ ): 1048 (vs), 962 (vs), 876 (s), 820 (sh), 798 (vs), 610 (m), 588 (m). The FAB mass spectrum was the same, within experimental error, as that for (TBA) $_4\text{H}_2[\text{Nb}_3\text{PW}_9\text{O}_{40}]$  (TBA2) (see below). Finke and Droege noted the same difficulty for the analogous Si-based system; i.e.,  $[(\text{NbO}_2)_3\text{SiW}_9\text{O}_{37}]^{7-}$  and  $[\text{Nb}_3\text{SiW}_9\text{O}_{40}]^{7-}$  gave very similar FAB mass spectra (oxygen is lost from the molecular ion). Anal. Calcd for (TBA) $_4\text{H}_2[(\text{NbO}_2)_3\text{PW}_9\text{O}_{37}]$ : C, 21.4; H, 4.11; N, 1.57; P, 0.87; Nb, 7.79; W, 46.3. Found: C, 21.3; H, 4.21; N, 1.57; P, 0.86; Nb, 7.84; W, 46.4.

**Synthesis of (TBA) $_4\text{H}_2[\text{Nb}_3\text{PW}_9\text{O}_{40}]$  (TBA2).** TBA1 (5.0 g) was dissolved in 25.0 mL of acetonitrile. A solution (0.5 mL) of 20% (TBA)OH/water was added, and the solution was refluxed for 24 h. During this time, the solution lost almost all of its yellow color. A white precipitate, present after cooling to room temperature, was removed, and the filtrate volume was reduced by half. This solution was stored at 0 °C overnight. The pale yellow amorphous precipitate was collected and washed with small portions of cold acetonitrile to remove any traces of the much more soluble parent triperoxo complex. The yield was approximately 80%.  $^{31}\text{P}$  NMR:  $\delta$  -7.36. FTIR (1200–400  $\text{cm}^{-1}$ ): 1048 (vs), 962 (vs), 876 (s), 820 (sh), 798 (vs), 610 (m), 588 (m). The FAB-MS spectrum ( $m/z$  of main peak = 3575 amu) was consistent with a monomer. Anal. Calcd for (TBA) $_4\text{H}_2[\text{Nb}_3\text{PW}_9\text{O}_{40}]$ : C, 21.2; H, 4.06; N, 1.55; P, 0.85; Nb, 7.69; W, 45.7. Found: C, 21.3; H, 4.13; N, 1.56; P, 0.86; Nb, 7.78; W, 46.0.

**Synthesis of (TBA) $_3\text{H}_3[\text{Nb}_6\text{P}_2\text{W}_{18}\text{O}_{77}]$  (TBA3).** TBA2 (5.0 g) was dissolved in 30 mL of acetonitrile with stirring. A solution of glacial acetic acid in acetonitrile (5.0 mL, 6.0 M) was slowly added dropwise with continued stirring. The solution was allowed to stir for 15 min to ensure reaction completion. An acetonitrile solution (5.0 mL) containing 0.5 and 1.0 g of (TBA)HSO $_4$  and (TBA)Br, respectively, was prepared and added. Storage at 0 °C afforded a pale yellow amorphous powder in nearly quantitative yield.  $^{31}\text{P}$  NMR:  $\delta$  -6.78. Low solubility of TBA3 precluded acquisition of an acceptable  $^{183}\text{W}$  NMR spectrum of the complex. FTIR (1200–400  $\text{cm}^{-1}$ ): 1048 (vs), 962 (vs), 876 (s), 820 (sh), 798 (vs), 690 (s), 610 (m), 588 (m). FAB mass spectra also showed peaks characteristic of the monomer. The same difficulty in acquiring FAB-MS data on the isostructural Si-based compounds, namely that the monomer and dimer were altered under the conditions of the analysis and gave similar spectra, was also operable for the P-based compounds. Electron impact and MALDI mass spectra also failed to adequately distinguish between monomer and dimer. Anal. Calcd for (TBA) $_3\text{H}_3[\text{Nb}_6\text{P}_2\text{W}_{18}\text{O}_{77}]$ : C, 9.79; H, 1.90; N, 0.71; P, 1.05; Nb, 9.46; W, 56.2. Found: C, 9.74; H, 1.83; N, 0.70; P, 1.01; Nb, 9.59; W, 56.7.

**Quantification of Peroxonio niobium Groups with Triphenylphosphine.** To 25.0 mL of dry acetonitrile was added 5.0 g of TBA1. A second 20.0-mL dry acetonitrile solution was prepared containing 1.50 g of  $\text{PPh}_3$  (gentle heating may be necessary). This phosphine solution was added to the solution of TBA1 in 1.0 mL aliquots. The progress of the reaction (formation of triphenylphosphine oxide) was monitored by  $^{31}\text{P}$  NMR. Found:  $2.8 \pm 0.3$  active oxygen equiv/equiv of 1.

**X-ray Crystallography.** A single crystal of the cesium salt of 1, CsI, was prepared as follows.  $\text{K}_7[\text{HNb}_6\text{O}_{19}] \cdot 13\text{H}_2\text{O}$  (2.47 g, 1.80 mmol) was dissolved in 300 mL of 0.5 M aqueous hydrogen peroxide. To this stirred solution was added dropwise 24 mL of 1.0 M HCl to give a bright yellow solution to which 10.32 g (3.63 mmol) of solid  $\text{A-Na}_9[\text{PW}_9\text{O}_{34}]$  was added. When all the solid had dissolved, CsCl (20.20 g dissolved in 20 mL of water prior to addition) was added to give an orange yellow precipitate. The solid was isolated by suction filtration, washed with ether, and dried in air to give 7.14 g of a yellow powder (69.2% yield based on  $\text{PW}_9$ ). This product was recrystallized from deionized water by slow evaporation at ambient temperature to give well-formed yellow bar-shaped parallelogram crystals.  $^{31}\text{P}$  NMR ( $\text{D}_2\text{O}$ , + $\text{LiClO}_4$ , - $\text{CsClO}_4$ , filtrate pH = 5; 3 equiv of  $\text{H}_2\text{O}_2$  added before data acquisition):  $\delta$  -7.33 (s). FTIR (1100–400  $\text{cm}^{-1}$ ): 1044 (m), 978 (sh), 961 (m), 870 (sh), 799 (s), 670 (w), 606 (w), 581 (w), 513 (vw), 480 (vw), 430 (vw).

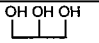
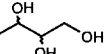
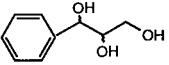
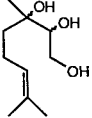
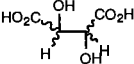
One representative well-formed crystal of  $\text{Cs}_6[(\text{NbO}_2)_3\text{PW}_9\text{O}_{37}] \cdot \text{HCl} \cdot 6.5\text{H}_2\text{O}$  (0.27  $\times$  0.07  $\times$  0.07 mm) coated with a thin layer of epoxy was mounted on a glass fiber and centered on a standard Siemens SMART CCD Area Detector System equipped with a normal-focus molybdenum-target X-ray tube. A total of 1271 frames of data were collected using a narrow-frame method with scan widths of 0.3° in  $\omega$  and an exposure time of 30 s/frame ( $2\theta_{\text{max}} = 56.40^\circ$ ). Frames were integrated with the Siemens SAINT program to yield a total of 31 690 reflections, of which 11 944 were independent ( $R_{\text{int}} = 8.18\%$ ,  $R_{\text{sig}} = 11.98\%$ ) and 6893 were above  $4\sigma(F)$ . The data were corrected for absorptions using Sheldrick's SADABS program. The corrected data were used for subsequent solution and refinement. The structure was solved by direct methods<sup>46</sup> and refined by full-matrix-least-squares-on- $F^2$  techniques (reflections with  $F^2 > 2\sigma(F_o^2)$ ), using anisotropic temperature factors for all the non-hydrogen atoms.<sup>47</sup> No attempt was made to place the hydrogen atoms on the water molecules of crystallization. Disorder in some of the cesium cations and water molecules was observed. Partial occupancies were used for several water molecules with higher temperature factors during the final stage of refinement. At final convergence,  $R_1 = 5.38\%$ ,  $wR_2 = 14.73\%$ , and GOF = 0.982 for 666 parameters. See the Supporting Information for crystal and data acquisition parameters (Table S1).

**Epoxidation of Alkenes in the Presence of 1 (Table 1).** In a typical reaction, 15 mmol of alkene substrate was added to acetonitrile (5 mL)

(46) Siemens Crystallographic Research Systems, Siemens Analytical X-ray Instruments, Inc., Madison, WI, 1990.

(47) Sheldrick, G. M. *SHELX 93: Program for structure refinement*; University of Goettingen: Goettingen, Germany, 1993.

**Table 1.** Oxidation of Various Alkenes by H<sub>2</sub>O<sub>2</sub> in the Presence of **1**<sup>a</sup>

Substrate	% Yield <sup>b</sup>	Reaction Time	Products <sup>c</sup>
Allyl alcohol	74	6.0h	
Crotyl alcohol <sup>d</sup>	94	1.0h	
Cinnamyl alcohol <sup>d</sup>	91	1.0h	
Geraniol <sup>d</sup>	94	1.0h	
Maleic acid <sup>d,e</sup>	56	12h	

<sup>a</sup> Substrate:oxidant:catalyst 100:150:1, in acetonitrile at reflux. All other specifics are given in the Experimental Section. <sup>b</sup> Defined as mmol of product/mmol of alcohol substrate. <sup>c</sup> Principal products only. Trace products (<1%) were not identified. <sup>d</sup> Stereoisomers not determined. <sup>e</sup> Additional acidity from the substrate results in a faster rate of peroxide disproportionation.

followed by 0.5 g of TBA1 (0.15 mmol) with stirring at room temperature. After the polyoxometalate was completely dissolved, the reaction was initiated by the addition of 2.5 mL of ca. 33% aqueous H<sub>2</sub>O<sub>2</sub>. The reaction vessel was then fitted with a condenser, and the reaction mixture was placed at reflux in a thermostated bath for the appropriate time (see Table 1 for reaction times). The vessel was then removed, rapidly cooled to room temperature, and an appropriate internal standard (trimethylacetonitrile or *n*-decane) was added. The reaction was assayed by gas chromatography. In control reactions with allylic alcohol as the substrate, 1.0 equiv (in one reaction) and 9.0 equiv (in a second reaction) of (TBA)<sub>2</sub>WO<sub>4</sub> were used in the place of TBA1 with all other reaction conditions the same in order to compare the catalytic activities. A control reaction with [Nb(O)<sub>2</sub>]<sub>4</sub><sup>3-</sup>, a model for Nb resulting from decomposition of **1** during reaction, was also assessed.

**Kinetic Studies. Allylic Alcohol Epoxidation in the Presence of 1.** In a typical reaction, the appropriate amount of catalyst precursor, TBA1, was added to a 5-mL round-bottom flask containing 2.0 mL of acetonitrile, 0.41 mL of allylic alcohol, substrate, and 25  $\mu$ L of *p*-xylene, internal standard. The reaction was initiated by the addition of 1.0 mL of ca. 33% aqueous H<sub>2</sub>O<sub>2</sub>, and the mixture was placed at reflux for 100 min. The disappearance of alkene substrate was monitored by removal of small aliquots of the reaction mixture at 20-min intervals and acquisition of the <sup>1</sup>H NMR spectra of each.

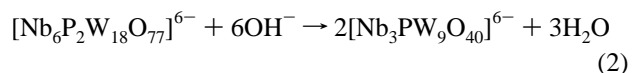
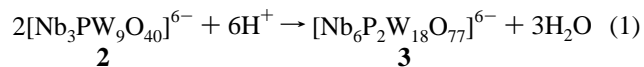
For the incubation study, the catalyst precursor, TBA1 (30  $\mu$ mol), was dissolved in 2.0 mL of acetonitrile, and the solution was placed at reflux. After the appropriate reaction time had elapsed, the reaction was initiated by the addition of a freshly prepared solution consisting of 0.41 mL of allylic alcohol, 25  $\mu$ L of *p*-xylene, and 1.0 mL of ca. 33% aqueous H<sub>2</sub>O<sub>2</sub>. This solution was maintained at reflux for 100 min. The initial rates were determined by <sup>1</sup>H NMR by following the disappearance of the alkene substrate.

## Results and Discussion

**Synthesis and Characterization of the Triniobium Substituted Polytungstophosphates.** The tris(peroxoniobium)

complex [(NbO<sub>2</sub>)<sub>3</sub>PW<sub>9</sub>O<sub>37</sub>]<sup>6-</sup> (**1**), the corresponding POM, [Nb<sub>3</sub>PW<sub>9</sub>O<sub>40</sub>]<sup>6-</sup> (**2**), and its dimer, [Nb<sub>6</sub>P<sub>2</sub>W<sub>18</sub>O<sub>77</sub>]<sup>6-</sup> (**3**), were all prepared, purified, and characterized. Details can be found in the Experimental Section, and key points are elaborated below. The spectroscopic, titrimetric, and elemental analysis data are all consistent with these formulas. Some of this chemistry is quite similar to that of the analogous silicon compounds reported by Finke and co-workers.<sup>3,6</sup> The terminal  $\eta^2$ -O<sub>2</sub><sup>2-</sup> groups on the Nb atoms in TBA1 decompose to the corresponding oxo groups in CH<sub>3</sub>CN solution. These oxo groups convert back to the terminal peroxy groups upon addition of 10% v/v 33% H<sub>2</sub>O<sub>2</sub> in CD<sub>3</sub>CN. At the same time, the presence of H<sub>2</sub>O<sub>2</sub> over a longer period appears to decompose the polytungstate unit. Both the reconstitution of the terminal peroxy units on Nb<sup>V</sup> centers in POMs<sup>27</sup> and the peroxolytic degradation of polytungstophosphates<sup>28,31,32,34</sup> are preceded chemical processes. These H<sub>2</sub>O<sub>2</sub>-based reactions render the acquisition of impurity-free NMR spectra of **1** in solution problematical. The <sup>31</sup>P NMR and <sup>183</sup>W NMR spectra of TBA1 are given in Figure 1.

The reaction of K<sub>7</sub>[HNb<sub>6</sub>O<sub>19</sub>], aqueous H<sub>2</sub>O<sub>2</sub>, and A-Na<sub>9</sub>[PW<sub>9</sub>O<sub>34</sub>] in water followed by treatment with (TBA)Br and then reprecipitation under two sets of conditions reproducibly affords the TBA salt of the tris(peroxoniobium) heteropolyanion [(NbO<sub>2</sub>)<sub>3</sub>PW<sub>9</sub>O<sub>37</sub>]<sup>6-</sup> (**1**) in ~60% isolated yield. Peroxide titration by triphenylphosphine implicates 2.8  $\pm$  0.3 peroxide groups per molecule, close to the theoretical value of 3.0. The best preparation of the corresponding POM, [Nb<sub>3</sub>PW<sub>9</sub>O<sub>40</sub>]<sup>6-</sup> (**2**), involves refluxing **1** in acetonitrile for 24 h. This refluxing is conducted in the presence of a soluble form of hydroxide to prevent dimerization of **2** to [Nb<sub>6</sub>P<sub>2</sub>W<sub>18</sub>O<sub>77</sub>]<sup>7-</sup> (**3**). The yield of **2** based on **1** after isolation and purification is 80%. Interconversions of the monomer, **2**, and the dimer, **3**, are analogous to those of the corresponding Si compounds (eqs 1 and 2).<sup>5</sup> Treatment of **2** with glacial acetic acid in acetonitrile



converts it to **3** in nearly quantitative yield, eq 1. Treatment of **3** with hydroxide converts it back to **2** in very high yield. The titration curve for eq 2 (the intensity of the Nb–O–Nb stretching fundamental in the mid-infrared at 687 cm<sup>-1</sup> versus the equivalents of hydroxide added per equivalent of **3**) shows no change until between 2 and 3 equiv of hydroxide is consumed. This is consistent with the removal of two or three protons associated with **3** prior to cleavage of the Nb–O–Nb bonds. The elemental analysis for **3** clearly indicates the presence of three protons (three TBA cations) per molecule in the yellow solid obtained from acetonitrile.

The structures of the trivacant silicon-based Keggin fragments and complexes of these fragments have been unequivocally characterized in large part by multiple efforts over a period of years by the Finke and Tézé groups.<sup>3,4,6,48,49</sup> There are two pertinent types of isomerism in trivacant Keggin fragments and for PW<sub>9</sub> species. The first type of isomerism involves the pattern of the W units removed from the parent Keggin complex

(48) Canny, J.; Tézé, A.; Thouvenot, R.; Hervé, G. *Inorg. Chem.* **1986**, *25*, 2114–2119.

(49) Tézé, A.; Hervé, G. In *Inorganic Synthesis*; Ginsberg, A. P., Ed.; John Wiley and Sons: New York, 1990; Vol. 27; pp 85–96.

(alternatively, a substitutional isomerism), and two types of unit removal isomers have been documented in  $PW_9$  species: A type, which results from W units removed from three different  $W_3O_{13}$  units, and B type, which results from one  $W_3O_{13}$  unit removed.<sup>1</sup> The second type of isomerism involves  $\pi/3$  rotation of the capping  $W_3$  unit in trivacant fragments and two types are the most prevalent:  $\alpha$ , in which no rotation from the parent Keggin complex of maximal symmetry is observed, and  $\beta$ , in which one  $W_3$  group has been rotated by  $\pi/3$  rad.<sup>1</sup> In principle, all four isomers of  $PW_9$  are possible, A, $\alpha$ , A, $\beta$ , B, $\alpha$ , and B, $\beta$ , although Pope has noted that B, $\beta$  is unlikely as it violates the Lipscomb rule.<sup>50</sup> Droege and Finke first determined the unit removal isomerism in  $PW_9$ . They demonstrated via the synthesis of crystallographically characterized B- $P_2W_{18}M_4$  complexes that  $PW_9$  (most likely an A isomer) was transformed by heating to B- $PW_9$ . Later, Knoth and co-workers used the solid state infrared spectrum, primarily on the basis of the strength of the P=O(OH) stretch, and the chemical shift anisotropy from the solid state  $^{31}P$  NMR spectra (MAS and non-spinning) to make a defensible absolute assignment of the precursor as an A isomer.<sup>51</sup> Additional research by Finke and co-workers on the B- $PW_9$  type dimeric transition metal complexes further clarified the A versus B isomerism in  $PW_9$  units.<sup>52</sup> The confirmation of the A versus B assignment came from the X-ray crystal structures of the complexes  $[(CeO)_3(PW_9O_{34})_2]^{12-}$  and  $[Cu_3(PW_9O_{34})_2]^{12-}$  (high-quality data sets) and  $[Ni_3(PW_9O_{34})_2]^{12-}$  (lower quality data set) by Knoth and co-workers.<sup>53</sup> These complexes were prepared from unheated  $PW_9$ , and all three were A, $\alpha$  isomers. More recently, the X-ray structure of another dimer based on A-type trivacant Keggin units was reported by Wassermann et al., the complex  $[\{A,\alpha-Cr_3SiO_4W_9O_{30}(OH)_3\}_2(OH)_3]^{11-}$ .<sup>54</sup>

**X-ray Structure of 1 and Clarification of Isomerism.** The rotational isomerism of the  $M_3$  unit ( $\alpha$  versus  $\beta$ ) in **1–3** was the main uncertainty in this research. The first definitive investigation of rotational isomerism in  $PW_9$  (and  $AsW_9$ ) was that of Contant et al. in 1974.<sup>55</sup> Since then, two groups have reported three X-ray structures of POMs that contain the A, $\beta$ - $PW_9$  unit: A, $\beta$ - $[N(CH_3)_4]_3[PMo_3W_9O_{40}]$  by Kawafune and Matsubayashi in 1992,<sup>56</sup>  $K_5H_4[(PhSn)_3P_2W_{15}O_{59}]$  by Xin and Pope in 1994,<sup>57</sup> and A, $\beta$ - $Cs_{5.4}H_{0.6}[PV_3W_9O_{40}]$  by Kawafune et al. in 1997.<sup>58</sup>

No spectroscopic technique, including vibrational spectroscopy, unequivocally characterizes this cap rotational isomerism. Rocchiccioli-Deltcheff argued that the vibrational spectra of the common Keggin  $\alpha$  and  $\beta$  isomers should differ in the regions characteristic of the corner-shared M–O–M vibrations, since all the other bonds remain unchanged.<sup>59</sup> Extensive vibrational studies (both FTIR and Raman spectra) conducted in our laboratory, however, failed to provide compelling evidence for either A, $\alpha$  or A, $\beta$  units in these three triniobium-substituted POMs.

(50) Lipscomb, W. N. *Inorg. Chem.* **1965**, *4*, 132–134.

(51) Knoth, W. H.; Domaille, P. J.; Farlee, R. D. *Organometallics* **1985**, *4*, 62–68.

(52) Finke, R. G.; Droege, M. W.; Domaille, P. J. *Inorg. Chem.* **1987**, *26*, 3886–3896.

(53) Knoth, W. H.; Domaille, P. J.; Harlow, R. L. *Inorg. Chem.* **1986**, *25*, 1577–1584.

(54) Wassermann, K.; Palm, R.; Lunk, H.-J.; Fuchs, J.; Steinfeldt, N.; Stoesser, R. *Inorg. Chem.* **1995**, *34*, 5029–5036.

(55) Contant, R.; Fruchart, J.-M.; Hervé, G.; Tézé, A. C. R. *Acad. Sci. Paris, Ser. C* **1974**, *278*, 199–202.

(56) Kawafune, I.; Matsubayashi, G. E. *Chem. Lett.* **1992**, 1869–1872.

(57) Xin, F. B.; Pope, M. T. *Organometallics* **1994**, *13*, 4881–4886.

(58) Kawafune, I.; Tamura, H.; Matsubayashi, G. *Bull. Chem. Soc. Jpn.* **1997**, *70*, 2455–2460.

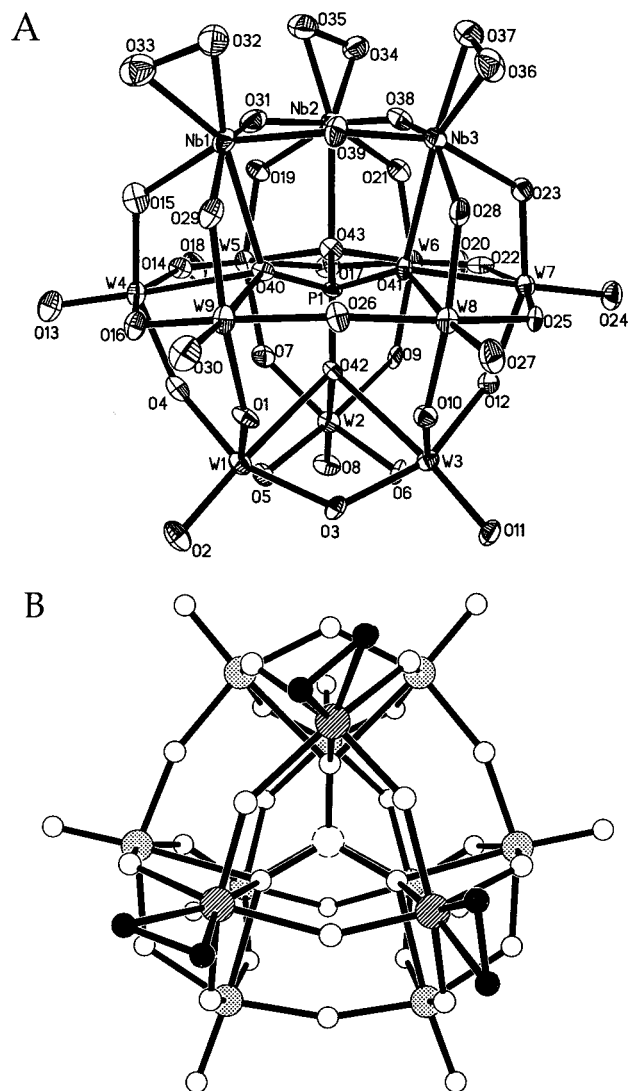


**Figure 2.** (A) ORTEP drawing of the polyanion A, $\beta$ - $[(NbO_2)_3PW_9O_{37}]^{6-}$  (**1**) (side view). (B) Ball-and-stick drawing (top view) showing the approximate  $C_3$  orientation of the three terminal peroxo groups.

Finally, the preparation of crystallographically tractable cesium derivatives was achieved, and a dataset for  $Cs_6[(NbO_2)_3PW_9O_{37}] \cdot HCl \cdot 6.5H_2O$  (**Cs1**) collected on a CCD-equipped diffractometer facilitated structure elucidation of **1**. The monoclinic space group ( $P2/c$ ) and a disorder-free Keggin unit provided a straightforward solution of structure and refinement. Full details of crystal, data collection, and refinement information are provided in the Experimental Section or in the Supporting Information. A combined ORTEP plot and atom-numbering diagram of **1** is given in Figure 2A, and a ball-and-stick diagram (top view down the approximate 3-fold axis) is given in Figure 2B.

The X-ray structure establishes that **1** contains A, $\beta$ - and not the A, $\alpha$ - $PW_9$  units. Figure 2 confirms that **1** is a tris-(peroxoniobium)-substituted Keggin derivative, which is consistent with the stoichiometry used in the synthesis. Each of the three Nb atoms belongs to three different edge-shared  $NbW_2O_{13}$  groups and each is linked to the other through the corner sharing (the A-type positional isomer). The fourth edge-

(59) Thouvenot, R.; Fournier, M.; Franck, R.; Rocchiccioli-Deltcheff, C. *Inorg. Chem.* **1984**, *23*, 598–605.

shared  $W_3O_{13}$  group is rotated by  $60^\circ$  about the 3-fold axis from the  $\alpha$  isomer, which defines the  $\beta$  isomer.

The data unequivocally distinguish and define the Nb and W atoms. The observed electron densities on the Nb and W atoms are quite different. Refinements using the W atomic scattering factor<sup>60</sup> for the Nb positions do not converge with satisfactory temperature factors. Each of the three Nb atoms is ligated by four doubly bridged O atoms, one quadruply bridged O atom, and one terminal  $\eta^2$ -coordinated peroxy unit to define a distorted pentagonal bipyramidal coordination polyhedron. The nine W atoms all exhibit conventional octahedral coordination polyhedra. Such pentagonal bipyramidal coordination polyhedra containing the  $\eta^2$ -peroxy unit is seen for metal centers in only two other structurally characterized conventional highly condensed polyanions, the  $\beta_3$ - $[(Co^{II}O_4)W_{11}O_{31}(O_2)_4]^{10-}$  complex of Baker and co-workers<sup>61,62</sup> and the  $\alpha$ - $[(NbO_2)_6P_2W_{12}O_{56}]^{12-}$  complex of Hill and co-workers.<sup>27</sup> The average  $O_p-O_p$  distance in the polyanion (1.51 Å) is longer than those reported for  $\alpha$ - $[(NbO_2)_6P_2W_{12}O_{56}]^{12-}$  (average 1.43 Å) and the noncoordinated  $O_2^{2-}$  (average 1.49 Å),<sup>63</sup> and the average  $O_p-Nb-O_p$  angle of  $45.2^\circ$  is also larger than those of  $\alpha$ - $[(NbO_2)_6P_2W_{12}O_{56}]^{12-}$  (average  $43.7^\circ$ ) and the  $[Nb(O_2)_4]^{3-}$  (average  $43.3^\circ$ ). The average Nb- $O_p$  distance of 1.96 Å is also slightly longer than those of  $\alpha$ - $[(NbO_2)_6P_2W_{12}O_{56}]^{12-}$  (average 1.93 Å) and the  $[Nb(O_2)_4]^{3-}$  (average 1.94 Å). The other distances (W-O, Nb-O, and P-O) are in the normal range (see Supporting Information).

The relative orientation of the Nb( $O_2$ ) units is noteworthy. Each  $\eta^2$ -peroxy moiety lies in a plane defined by  $Nb_2W_4$ , and the relative orientations of the three  $Nb_2W_4$  planes at ca.  $120^\circ$  angles to each other give the polyanion approximately  $C_3$  symmetry. The arrangements of these  $\eta^2$ -peroxy groups likely derive from interactions between peroxy group p orbitals and niobium d orbitals and to a lesser extent from cation-anion interactions in the crystal lattice. Knoth has documented that, in aqueous solutions at pH 1–3,  $A,\alpha$ -PW<sub>9</sub> can form  $[(WO_2)_2-(PW_9O_{34})_2]^{14-}$  and, upon heating,  $[(WO_2)_3(A,\alpha-PW_9O_{34})_2H_6]^{6-}$ .<sup>53</sup> There is no evidence for the existence of these species during the conversions of the triperoxy complex to the corresponding trioxo complex (**1** to **2**) or for hydroxide cleavage of dimer back to monomer, eq 2 (**3** to **2**), under the conditions in these studies (aprotic media etc.; see Experimental Section).

**H<sub>2</sub>O<sub>2</sub>-Based Epoxidation of Alkenes by  $[(NbO_2)_3PW_9O_{37}]^{6-}$ , **1**.** The tris(peroxoniobium) complex, **1**, added to acetonitrile solutions of alkenes and aqueous H<sub>2</sub>O<sub>2</sub> results in the dihydroxylation of the alkene units in high selectivities at moderate to high conversions of substrate. Exemplary data are summarized in Table 1. The product distributions are similar to those from the  $[(NbO_2)_3SiW_9O_{37}]^{7-}/H_2O_2/alkene$  system investigated by Droege and Finke.<sup>5</sup> The H<sub>2</sub>O<sub>2</sub> consumed was evaluated titrimetrically in representative reactions, and typically 20–30% was lost to disproportionation during reaction. The acidity of these nonaqueous catalytic solutions was estimated by two methods as described in the Experimental Section and corresponds to an approximate pH of 2. At such pH values, two phenomena pertinent to the reactions require comment. First,

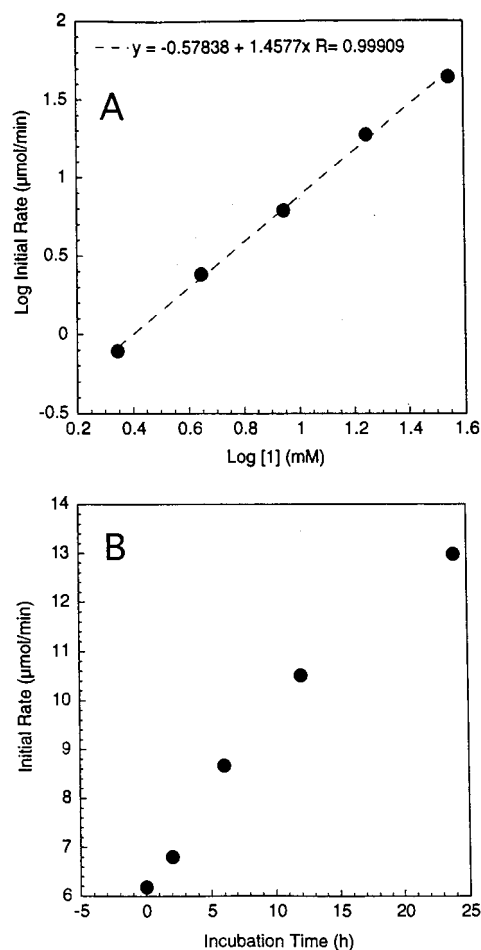


**Figure 3.** Kinetics of the epoxidation of allylic alcohol in the presence of **1**: (A) van't Hoff log-log plot of the rate dependence ( $-d[\text{allylic alcohol}]/dt$ ) on the initial concentration of **1**; (B) comparison of the initial rate of epoxidation as a function of catalyst incubation time before reaction (see text).

acid-catalyzed alkene oxidation by H<sub>2</sub>O<sub>2</sub> could be quite fast. This rate was evaluated experimentally under reaction conditions identical to those in Table 1 and found to be unimportant ( $<0.3 \mu\text{M}/\text{min}$ ). Second, acid-catalyzed ring opening of epoxides to form the vicinal diols can be anticipated. A rate for the control reaction of authentic glycidol (allyl alcohol epoxide) to glycerol ( $-d[\text{glycidol}]/dt$ ) was also evaluated, and the initial rate of epoxide ring opening was found to be much faster (more than an order of magnitude) than that for allyl alcohol oxidation under these reaction conditions. This significantly faster rate of epoxide ring opening to epoxide generation is consistent with the lack of epoxide products in Table 1.

The identity of the real catalytic species in these H<sub>2</sub>O<sub>2</sub> oxidations was of interest, given that solid literature studies substantiate that POMs can function either as epoxidation catalyst precursors (again, usually d<sup>0</sup> complexes)<sup>28–36</sup> or as intact catalysts themselves (again, usually d-electron transition metal substituted complexes; see Introduction).<sup>37–40</sup> Furthermore,  $WO_4^{2-}$  is well documented to catalyze epoxidation by H<sub>2</sub>O<sub>2</sub>, affording product distributions similar to those in Table 1.<sup>64</sup> Complex **1** clearly breaks down during reaction with H<sub>2</sub>O<sub>2</sub> and alkenes. The identity of the active catalyst species when **1** is added to solutions containing alkenes and H<sub>2</sub>O<sub>2</sub> was probed by four experiments using allyl alcohol as a representative substrate. Unless otherwise stated, the reaction conditions in these control

(60) Cromer, D. T.; Waber, J. T. *International Tables for X-ray Crystallography*; Kynoch Press: Birmingham, England, 1974; Vol. IV, Table 2.2B.

(61) Dickman, M. H.; Pope, M. T. *Chem. Rev.* **1994**, *94*, 569–584.

(62) Bas-Serra, J.; Todorut, I.; Jameson, G. B.; Acerete, R.; Baker, L. C. W. *Abstracts of Papers*, International Chemical Congress of Pacific Basin Societies, Honolulu, HI, 1989; American Chemical Society: Washington, DC, 1989.

(63) Vaska, L. *Acc. Chem. Res.* **1976**, *9*, 175–183.

(64) Raciszewski, Z. *J. Am. Chem. Soc.* **1960**, *82*, 1267–1277.

and investigatory experiments were identical to those of the parent reaction itself given in the Experimental Section and the footnotes of Table 1. First, there is a linear correlation (99.9 correlation coefficient for a five-point fit) between the log of the initial rate of consumption of substrate and the log of the initial concentration of **1** (a 15-fold concentration range). This yields a fraction order, 1.46, in **1** (Figure 3A). Second, the  $^{31}\text{P}$  NMR spectrum after reaction shows multiple phosphorus-containing species, with **1** representing 86% of the total phosphorus in the sample ( $\text{PO}_4^{3-}$  accounted for  $\sim 5\%$  of the total phosphorus).  $^{183}\text{W}$  NMR could not be used to quantify the decomposition of **1** as the data collection time was longer than the decomposition time. Third, the activities of 9 equiv of  $\text{WO}_4^{2-}$  and 3 equiv of the Nb peroxy monomer, which model the complete breakdown of **1** in situ, were both assessed and compared to the reactivity of **1**. The conversions of allyl alcohol starting with 1 equiv of **1**, 1 equiv of the Nb peroxy species  $\text{Nb}(\text{O}_2)_4^{3-}$ , 1 equiv of  $\text{WO}_4^{2-}$  (the acetonitrile-soluble TBA salt), and 9 equiv of  $(\text{TBA})_2\text{WO}_4$  are 7.5%, 4% (detectable limit is  $<0.2\%$ ), 11%, and 33%, respectively. The fourth and most important experiment, summarized in Figure 3B, kinetically assesses the importance of the decomposition of **1** under the reaction conditions and provides key information. Here **1** was incubated in the reaction medium and under conditions (refluxing acetonitrile) without  $\text{H}_2\text{O}_2$  for five varying times and the kinetics of allyl alcohol oxidation by  $\text{H}_2\text{O}_2$  was evaluated at each of these times. The five initial rates vary directly with the incubation time. There are two clear inferences from this

novel experiment and the plot in Figure 3B. First, the extrapolation to zero incubation time implicates some activity for **1** itself. A similar inference cannot be drawn from the data of Droege and Finke on the corresponding  $[(\text{NbO}_2)_3\text{SiW}_9\text{O}_{37}]^{7-}/\text{H}_2\text{O}_2$  system. Second, it is clear for **1**, as for the  $[(\text{NbO}_2)_3\text{SiW}_9\text{O}_{37}]^{7-}/\text{H}_2\text{O}_2$  system, that species other than the intact starting POM are the dominant catalysts. The collective data, including those for the  $\text{WO}_4^{2-}/\text{H}_2\text{O}_2$ /substrate control experiments, are consistent with  $\text{WO}_4^{2-}$  itself being the dominant catalyst in both the  $\text{XW}_9$ ,  $\text{X} = \text{P}(\text{V})$ , and  $\text{Si}(\text{IV})/\text{H}_2\text{O}_2$  systems.

**Acknowledgment.** We thank the National Science Foundation (Grant CHE-9412465), the National Institutes of Health (Grant R01 AI32903-04A1), and the Molecular Design Institute (Office of Naval Research Grant N00014-95-1-1116) for support. We also thank Dr. Mark Mitchell for the use of his Raman equipment and Jennifer Cowan for collecting the  $^{183}\text{W}$  NMR data shown in Figure 1.

**Supporting Information Available:** Tables listing crystal data and structure determination details, atomic coordinates and equivalent isotropic displacement coefficients, bond lengths and bond angles, and anisotropic displacement parameters for **Cs1**,  $\text{Cs}_6[\text{P}(\text{NbO}_2)_3\text{W}_9\text{O}_{37}]\cdot\text{HCl}\cdot 6.5\text{H}_2\text{O}$ , and figures showing  $^{31}\text{P}$  NMR spectra of **2** and **3** and kinetics plots for allyl alcohol oxidation by  $\text{H}_2\text{O}_2$  catalyzed by **TBA1**,  $\text{Nb}(\text{O}_2)_4^{3-}$ , and  $(\text{TBA})_2\text{WO}_4$  (20 pages). An X-ray crystallographic file for **Cs1**, in CIF format, is available on the Internet only. Ordering and access information is given on any current masthead page.

IC980467Z